Title

Radiomics for Response and Outcome Assessment for Non-Small Cell Lung Cancer.

Authors

Shi, Liting
He, Yaoyao
Yuan, Zilong
et al.

Publication Date

2018

DOI

10.1177/1533033818782788

Peer reviewed

Technology in Cancer Research & Treatment
Volume 17: 1-14

DOI: 10.1177/1533033818782788
journals.sagepub.com/home/tct
SAGE

Radiomics for Response and Outcome Assessment for Non-Small Cell Lung Cancer

Liting Shi, MS[1], Yaoyao He, BS[1], Zilong Yuan, BS[2], Stanley Benedict, PhD[3], Richard Valicenti, MD[3], Jianfeng Qiu, PhD[1], and Yi Rong, PhD[3]

Abstract

Routine follow-up visits and radiographic imaging are required for outcome evaluation and tumor recurrence monitoring. Yet more personalized surveillance is required in order to sufficiently address the nature of heterogeneity in nonsmall cell lung cancer and possible recurrences upon completion of treatment. Radiomics, an emerging noninvasive technology using medical imaging analysis and data mining methodology, has been adopted to the area of cancer diagnostics in recent years. Its potential application in response assessment for cancer treatment has also drawn considerable attention. Radiomics seeks to extract a large amount of valuable information from patients' medical images (both pretreatment and follow-up images) and quantitatively correlate image features with diagnostic and therapeutic outcomes. Radiomics relies on computers to identify and analyze vast amounts of quantitative image features that were previously overlooked, unmanageable, or failed to be identified (and recorded) by human eyes. The research area has been focusing on the predictive accuracy of pretreatment features for outcome and response and the early discovery of signs of tumor response, recurrence, distant metastasis, radiation-induced lung injury, death, and other outcomes, respectively. This review summarized the application of radiomics in response assessments in radiotherapy and chemotherapy for non-small cell lung cancer, including image acquisition/reconstruction, region of interest definition/segmentation, feature extraction, and feature selection and classification. The literature search for references of this article includes PubMed peer-reviewed publications over the last 10 years on the topics of radiomics, textural features, radiotherapy, chemotherapy, lung cancer, and response assessment. Summary tables of radiomics in response assessment and treatment outcome prediction in radiation oncology have been developed based on the comprehensive review of the literature.

Keywords

chemotherapy, NSCLC, radiomics, radiotherapy, response assessment, systemic therapy

Abbreviations

AUC, area under the receiver operating characteristic curve; AUC-CSH, area under the curve of the cumulative SUV-volume histogram; CRT, chemoradiotherapy; CT, computed tomography; DFS, disease-free survival; DM, distant metastasis; DMFS, distant metastasis–free survival; DSS, disease-specific survival; EGFR, epidermal growth factor receptor; FPR, false-positive rate; FNR, false-negative rate; GGO, ground-glass opacity; GTV, gross tumor volume; HU, Hounsfield unit; ICC, intraclass correlation coefficient; IVH, intensity–volume histogram; Law's, Law's texture measures; LoG, Laplacian transform of Gaussian filter; LR, local

[1] Department of Radiology, Taishan Medical University, Tai'an, China
[2] Department of Radiology, Hubei Cancer Hospital, Wuhan, China
[3] Department of Radiation Oncology, University of California Davis Comprehensive Cancer Center, Sacramento, CA, USA

Corresponding Authors:
Yi Rong, PhD, Department of Radiation Oncology, University of California Davis Comprehensive Cancer Center, 4501 X Street, Sacramento, CA 95817, USA.
Email: yrong@ucdavis.edu
Jianfeng Qiu, PhD, Department of Radiology, Taishan Medical University, No. 619, Changcheng Road, Taian, Shandong 271016, China.
Email: jfqiu100@gmail.com

recurrence; LRC, local-regional control; LRFS, locoregional recurrence-free survival; LRR, locoregional recurrence; MTV, metabolic tumor volume; NSCLC, non-small cell lung cancer; OS, overall survival; PET, positron emission tomography; PFS, progression-free survival; R^2, coefficient of determination; RECIST, The Response Evaluation Criteria in Solid Tumors; RI, retention index; RILI, radiation-induced lung injury; ROI, region of interest; RT, radiotherapy; *r*s, Spearman rank correlation coefficient; SBRT, stereotactic body radiotherapy; SD, standard deviation; SUV, standardized uptake value; SUV_{max}, maximum standardized uptake value; SUV_{mean}, mean standardized uptake value; SUV_{peak}, average of the voxel with SUV_{max} of the tumor region.

Received: November 13, 2017; Revised: March 09, 2018; Accepted: May 16, 2018.

Introduction

Lung cancer is one of the most common cancer in the world, accounting for the first place in men (16.7%) and third in women (8.7%).[1] When cancer is suspected, further confirmation and follow-up are required in order to assist clinicians with accurate diagnosis and develop properly indicated treatment regimens. Tumor biopsy and physiology analysis are the most accurate way for diagnosis. Yet biopsy has limitations, that is, the location of tumor biopsied may strongly affect physiology results.[2] Medical imaging systems are noninvasive approaches for tumor assessment and they provide substantial benefits, that is, tumor's biological and functional information and its surrounding microenvironment,[3] beyond simple tumor visualization with newly developed contrast and tracer agents. Diagnostic interpretation of medical images has become more sophisticated and focused on disease types. For instance, most tumors exhibit heterogeneity, both spatially and temporally, which can be visualized and tracked with new radiomics applications on chest radiographs and computed tomography (CT) images. Lambin *et al*[4] was the first to introduce the concept of "radiomics" in 2012 and presented its key technique and application prospects. Kumar *et al*[5] further expanded the definition and analyzed the challenges of each step of its workflow, especially for lung cancer in the same year. Radiomics is essentially derived from the concept of computer-aided diagnosis, which uses computer assistance in processing a large number of imaging features extracted from various imaging modalities, including CT, positron emission tomography (PET), magnetic resonance imaging, and/or other medical imaging modalities.[4,5] This strategy transforms the regions of interest (ROIs) into high-resolution, minable data by introducing the big data technology and using automatic data feature algorithms.[5] Adopted from radiology, this technique has been recently explored in cancer treatments, including tumor targeted drug therapy,[6] preoperative assessment of tumor surgery,[7,8] and response and outcome assessments after radiotherapy and systemic therapy.[9-13]

The applications of radiomics for non-small cell lung cancer (NSCLC) include (1) treatment efficacy and response evaluation, (2) to assist noninvasive early diagnosis, and (3) prediction of treatment outcomes. It becomes possible to detect tumor occurrence at an early stage, as well as to predict treatment efficacy and detect recurrence or metastasis after a given treatment regime of radiation and/or systemic therapy.[9,14] With the established database, care providers can now more practically predict treatment outcomes and possible radiation-induced injuries and seek out personalized and precise treatment options for patients.[15]

Previous review articles have provided summaries of radiomics analysis approaches, mathematical algorithms, and clinical applications in diagnosis, prognosis, or outcome predictions.[5,16-18] In 2014, Mattonen *et al*[10] reviewed novel techniques focusing on quantitative imaging feature analysis for response assessment after radiotherapy for lung cancer. In 2016, Parekh and Jacobs[17] summarized approaches and mathematical algorithms applied to lung, breast, liver, and so on. The development of radiomics and its application have also been discussed in various aspects.[19-21] More recently, several papers reviewed related texture analysis applied to PET/CT images for tumor response assessment[16,22,23] in the past 2 years. Scrivener *et al*[2] and Lee *et al*[18] focused on the application to lung cancer, while Sollini *et al*[24] proposed harmonizing PET radiomics methods for their applications in NSCLC.

Radiomics currently plays an important role in providing a fundamental methodology for future personalized treatment and follow-up in the era of precision medicine. Our focus is to elaborate the specific applications of radiomics in the context of radiotherapy with or without systemic regimen for NSCLC and its current research developments using CT and PET images. A comprehensive literature search was conducted using the PubMed database to include papers published from the year of 2007 to present, with the keywords of radiomics, textural features, radiotherapy, systemic therapy, chemotherapy, lung cancer, and response assessment. Summary tables in response assessment and treatment outcome prediction in radiation oncology have been developed based on the comprehensive review of the literature.

The Workflow of Radiomics

The workflow of radiomics, as shown in Figure 1, includes (1) imaging acquisition/reconstruction, (2) ROI definition/segmentation, (3) image feature extraction, and (4) image feature selection and classification. Research interests have been

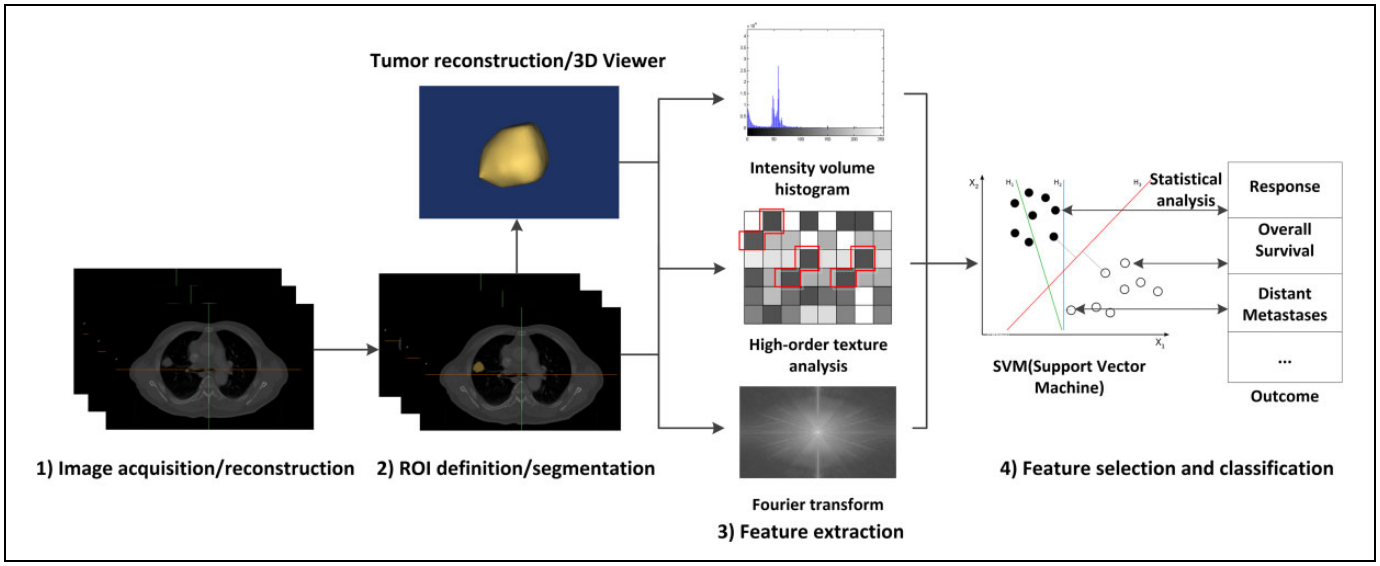

Figure 1. The workflow of radiomics.

widely focused on metrologies and challenges, as well as clinical applications of these aspects. Herein we describe in details various stages in the radiomics workflow.

Imaging Acquisition and Reconstruction

Acquiring high-quality and standardized images is a prerequisite for the accuracy and consistency of radiomics data. A large amount of the standardized image data can help establish a response assessment model to predict the probability of recurrence and metastasis after treatment.[6,25] Within those 2 commonly available types of image acquisition modalities for treating NSCLC, CT and PET, choosing a consistent image modality for the diagnosis and follow-up scans is essential to avoid divergence and discordance in the extracted feature data. In addition, even for the same imaging modality, the variations in acquisition parameters (kV, mAs, slice thickness, breathing control method, configurations, field strength, and contrast media) and reconstruction parameters (reconstruction kernels or filters) are likely to affect image values for scanning the exact same subject, which might complicate the process of ROI-based image segmentation and feature extraction.[5,26-30] Thus, it is essential to maintain homogeneity in image scan protocols for a radiomics study.

Region of Interest Segmentations

Image segmentation for ROI creations is a crucial step, which directly affects the quality of subsequent feature extraction, thus affects the correctness and accuracy of research results.[20,31] Segmentation includes manual, semiautomatic, and automatic segmentations. Manual segmentation means that an experienced physician manually delineates the ROI on images, which is currently the most widely used method.[28,32] Manual segmentation has minimal needs in specialized algorithms but demands user specialty and experience. It is also time-consuming and can have significant intra- and interobserver variability, which may cause obstacles in big data analysis.[33] The automatic segmentation does not require manual intervention and functions through computer-aided automation with preset parameters. However, it relies on the accuracy of algorithms and their ability to differentiate ROIs from surrounding tissues. Semiautomatic segmentation takes advantages of both manual intervention and software automation, which makes it a preferable method for radiomics data analysis.[5,14,19,34] Semiautomatic segmentation that uses computer segmentation method cannot be reliably used alone. Further manual intervention is needed to ensure the accuracy of segmentation.[35]

Reproducibility of quantitative PET and CT image features in NSCLC concerning variations caused by segmentation methods and patient factors had been studied and proved stable.[36-41] Several studies used intraclass correlation coefficient (ICC)[42] to compare the repeatability in manual, automatic, and semiautomatic segmentation methods.[36,38,39] Among them, Parmar *et al*[39] concluded that semiautomatic features provide higher reproducibility than manual segmentations (ICC: 0.85 ± 0.15 vs 0.77 ± 0.17). Semiautomatic multi-seed point segmentation can generate stable segmented volumes with similarity index above 0.93, compared to 0.73 in manual segmentation.[41] Overall, ROI identification and segmentation are critical factors in the process of imaging analysis and feature extraction.[43,44]

Image Feature Extraction

Exploring possible correlations between image feature information with tumors' phenotypes and prognostics is currently the main interest in radiomics research. Publications have shown potential diagnostic and prognostic powers from

Table 1. Features Extracted From PET and/or CT Images.

Class	Type	Method	Feature Name
Clinical factors	Age, gender, histology type, stage, etc		
Conventional features	PET only	SUV metrics	SUV_{mean}
			SUV_{max}
			SUV_{peak}
			COV
			SD
			AUC-SCH
		TLG	
		MTV	
	CT only	HU metrics	Mean
			Maximum
			COV
			SD
	PET/CT	Size, shape, volume, diameter, solidity, eccentricity, etc	
Texture features (PET/CT)	First order	IVH	Mean, variance, skewness, kurtosis, energy, entropy
		Law's	Level, edge, spot, wave, ripple
	High order	GLCM	Contrast, correlation, entropy, dissimilarity, energy, and so on
		GLRLM	Run percentage
			Short run emphasis
			Long run emphasis
			Gray-level nonuniformity
			Run-length nonuniformity
		GLSZM	Zone size percentage
			Zone size nonuniformity
			Gray-level nonuniformity, etc.
		NGTDM	Coarseness, contrast, busyness, complexity, texture strength
	Transform based	Wavelet, Fourier, LoG	

Abbreviations: AUC-CSH, area under the curve of the cumulative SUV-volume histogram; COV, coefficient of variation; CT, computed tomography; GLCM, gray-level co-occurrence matrix; GLRLM, gray-level run-length matrix; GLSZM, gray-level size zone matrix; HU, Hounsfield unit; IVH, intensity–volume histogram; Law's, Law's texture measures; LoG, Laplacian transform of Gaussian filter; MTV, metabolic tumor volume; NGTDM, neighborhood gray-tone difference matrix; PET, positron emission tomography; SD, standard deviation; SUV, standardized uptake value; SUV_{max}, maximum SUV; SUV_{mean}, average SUV; SUV_{peak}, peak SUV; TLG, total lesion glycolysiss.

radiomics signatures for lung patients.[45-50] Present literatures have reported clinical factors, conventional features, and texture features for radiomics or delta-radiomics studies.[19,45,51-56] Different from clinical factors and conventional features that are acquired from hospital records or radiology readings, texture features are calculated mathematically by software platforms, such as MATLAB or Python. Texture feature is the spatial distribution of gray-level intensity in images and analyzed by 2 main mathematical techniques in NSCLC: statistical methods and transform-based methods, of which the first one is most used for lung cancer.[6,16,32,45,51,57] More specific description of radiomics features are summarized in Table 1. Currently, one of the predictive models is established based on size, concavity, contour, and spiculation.[48] In fact, the size-based features can be good predictors of cancerous nodules by itself and has significant correlation with overall survival (OS).[46] Additionally, the diversity of image features, such as tumor's growth rate and volume change, and multivariate analysis can improve prediction accuracy.[46,51] It is even possible to determine benign or malignant lymph nodes status by using CT texture features.[49,50] More significant features are to be discovered and validated.

Feature Selection and Classification

Feature selection and classification are also crucial after extracting a large number of features, most of which may be noise or intercorrelated features. The procedure of selecting and classifying features is to reduce the dimension.[28,58] There are a few publications on comparing the abilities of different feature selection methods and machine learning classifying methods to predict outcomes for lung.[58,59]

Feature selection preserves a subset of useful and unique features, reducing the computational costs and increasing the accuracy of predation, which can be applied to supervised and unsupervised learning.[60,61] Previous research had demonstrated that Wilcoxon selection method had highest performance in supervised learning,[62] while principal component analysis[58] had higher prediction performance than Wilcoxon (area under the receiver operating characteristic curve [AUC] = 0.70. vs 0.67) in unsupervised learning.[58] Feature selection algorithms, that is, filtering, wrapper, and embedded methods, have their merits and demerits.[60,63] The filtering methods are independent of the chosen predictors, with efficient numeracy and statistical scalability, which can reduce dimensionality

and overfitting compared to the wrapper and embedded methods.[63] Comparison of 14 filter feature selection methods indicated that Wilcoxon selection has the highest performance in predicting OS (AUC = 0.65 ± 0.02) with maximum stability (0.84 ± 0.05).[62]

Among the two feature classifications, that is, supervised and unsupervised classifiers, the former requires user to provide patients' radiomics features and outcomes as training data (ie, support vector machines, random forest, decision tree, neural networks, boosting, discriminant analysis, k-nearest neighbors, etc),[64-68] while the latter doesn't require outcome data (ie, consensus clustering, k-means clustering, hierarchical clustering, etc).[17] Parmar *et al*[62] and Zhang *et al*[58] proved that random forest classifier has the highest prediction performance in OS (AUC = 0.66 and 0.71).

Moreover, a combination of different feature selection methods and classifiers can achieve different prediction results. It was found that a combination of Wilcoxon selection model with random forest classifier has the best performance for predicting OS, while near-zero variance selection model combined with random forest classifier is appropriate for predicting recurrence (AUC = 0.76), and zero variance selection model with naive Bayes classifier is the best to predict death (AUC = 0.77), and mixture discriminant analysis classifier alone (AUC = 0.73) was best for predicting recurrence-free survival .[58] Identification of feature selection methods, classification methods, and analyzing tools is a crucial step for improving accuracy, stability, and performance of features for assessing response and predicting clinical outcomes. Radiomics is an emerging area, so does the development of feature selection and classification algorithms. The optimal method is still being developed based on clinical needs.

Radiomics in Response and Outcome Evaluation

Literature on applying radiomics to assess response and predict treatment outcome for lung is based on pretreatment images (Table 2) and follow-up images (Table 3). Pretreatment imaging radiomics is used to discover the association of quantitative features extracted from images taken prior to treatment with response and outcomes monitored upon treatment completion. The focus of these studies is on the ability of predicting prognosis from the pretreatment features.[8,52,74,75] Delta-radiomics is a method that compares the changes within those features extracted from pretreatment images and follow-up images during and/or after the treatment, in order to identify signs of recurrence, metastases, or other morality.[15,56,77,81,83] Positron emission tomography and CT images have been widely used for lung patients and thus are readily available for radiomic analysis. Positron emission tomography images provide molecular metabolic information and thus detect disease early, while CT provides anatomical characteristics. The end points mostly studied in PET images are Response Evaluation Criteria in Solid Tumors (RECIST)-based responses[12,13,79] and outcomes, such as recurrence,[52,53,69,78,81] distant metastases (DM),[57,69] and survival.[54,55,71,72] The end points in CT images focus on pathological response, mutation status, and distinguishing radiation-induced lung injury (RILI). The image features with high correlation to those end points are listed in Tables 2 and 3. Most of these study trials are retrospective, thus patients' images along with clinical outcome data are achieved from records of medical institutions or hospitals.

Tumor Response Assessments

Positron emission tomography images. Tumor response studied in PET images including stable disease and progress disease is assessed by the RECIST and divided into 3 types: complete response, partial response, and nonresponse.[12,13,79] The extracted features are pretreatment standardized uptake value (SUV) metrics, metabolic tumor volume (MTV), total lesion glycolysis, quantitative texture features, such as entropy, correlation, contrast, and uniformity, and "delta-radiomics." Among them, texture features outperformed others in predicting tumor response to treatment. Cook *et al*[12,13] showed that texture features measured by coarseness, contrast, and busyness presented strong correlations with RECIST response to chemoradiotherapy (CRT; $P = .004, .002, .027$), while SUV parameters showed none. Texture features reflecting reduced heterogeneity measured by first-order standard deviation (SD), entropy, and uniformity ($P < .01, = .001, = .001$) also presented a stronger correlation with RECIST response to erlotinib than SUV metrics. Dong *et al*[79] found that even though pretreatment features, such as coefficient of variation, MTV, and contrast (AUC = 0.781, 0.686, 0.804) had a predictive capability for response to CRT, early changes in texture features can better predict response with higher specificity (80%-83.6%) and sensitivity (73.2%-92.1%).

Computed tomography images. Different from RECIST responses studied in PET images, tumor response studied in CT images mainly focuses on pathological response, and treatment responses such as tumor response to radiation and epidermal growth factor receptor (EGFR) mutation status reflected gefitinib response.[6-8,86,87] In terms of predicting pathological response, pretreatment primary tumor sphericity, texture features, lymph node homogeneity, and changes in primary tumor volume, mass, histogram features, and texture features are potential predictors for patients with NSCLC after CRT, while primary tumor intensity variability and size zone variability are predictive for patients after tyrosine kinase inhibitor therapy.[7,86] It is also found that lymph node phenotype has a better performance in classifying pathologic complete response and gross residual disease than primary tumor.[7] A study tracked tumor response to radiation in daily CT images during radiotherapy course found that reductions in mean Hounsfield unit (HU) in gross tumor volume (GTV) had a strong correlation with accumulated GTV dose ($R^2 > 0.99$) and were significantly associated with survival rate.[87] In predicting EGFR mutation status and reflected gefitinib response, a pretreatment Law's

Table 2. Pretreatment Imaging Radiomics in Response Assessment and Treatment Outcome Prediction.

Studied Images	Treatment	Stage	N	Median Follow-Up (Months)	End Points	Image Parameter Related to Results (*P* Value, c-Index, AUC, HR, etc)	Reference
PET only	SBRT	I-IIA	45	21.4 months	LR	Entropy, correlation (AUC: 0.872, 0.816)	Pyka *et al*[69]
					DSS	Entropy (HR: 7.48, $P = .016$)	
	SBRT	I-II	63	27.1 months (32.1 months for survivals)	DSS	Textural feature dissimilarity (HR: 0.822, $P = .037$)	Lovinfosse et al[70]
					DFS	Textural feature dissimilarity (HR: 0.834, $P < .01$)	
					OS	None	
	SBRT	I	101	17 months	DM	A 2-features model (c-index: 0.71; $P < .0001$; HR: 4.8); combine radiomic signatures and histologic type (c-index: 0.8; $P < .0001$; HR: 6.9)	Wu *et al*[57]
	CRT	IB-III	53	21.2 months (25.6 months for OS)	RECIST–response	Coarseness, contrast, busyness ($P = .004$, .002, .027)	Cook *et al*[13]
					PFS	Coarseness, contrast, busyness ($P = .002$, .015, .01)	
					Local PFS	Coarseness, contrast, busyness ($P = .016$, .02, .006)	
					OS	Coarseness (*P*: .003)	
	CRT	III	116	47.8 months	PFS	SUV_{max}, AUC-CSH (HR: 0.25,3.35; 95% CI: 0.09–0.70, 1.79-6.28; $P = .008$, <.001);	Kang *et al* [54]
					LRFS	AUC-CSH (HR: 3.27; 95% CI: 1.54–6.94; $P = 0.002$)	
					DMFS	AUC-CSH (HR: 2.79; 95% CI: 1.42–5.50; *P*: .003)	
	CRT	IIB, III	201 (155 + 23 + 23)	22.6 months; 20.0 months; 6.2 months	OS	1 textural feature: SumMean ($P = .006$)	Ohri *et al*[71]
	CRT(192), RT(28)	I-IIIB	220	1.47 years (1.81 years for survival)	OS	Relative volume above 80% SUV (*P*: .05)	Carvalho *et al* 2013[55]
	RT	III	195	37 months	OS risk stratification	Combine quantitative features with conventional PET metrics (*P*: .18, c-index: 0.62)	Fried *et al*[72]
PET and CT	SBRT	IV	27	24 months (18.3 months for survival)	LRR	IVH-slope in PET, COV in CT (*rs:* 0.3426, −0.2665; $P = .0403$-.0871), PET-V_{80}, CT-$V_{70:}$(*r*s: 0.4854, 0.5908; $P = .0067$-.0013)	Vaidya *et al*[52]
					Local failure	CT-IVH (*r*s: 0.4530; $P = 0.0105$), PET-V_{80}, CT-$V_{70:}$(*r*s: 0.4854, 0.5908; $P = .0067$-.0013)	

(continued)

Table 2. (continued)

Studied Images	Treatment	Stage	N	Median Follow-Up (Months)	End Points	Image Parameter Related to Results (*P* Value, c-Index, AUC, HR, etc)	Reference
CT only	SBRT	I-II	113	20.8 months (25.2 months for survivals)	OS	Volume, diameter, and 2 radiomic features	Huynh *et al* [32]
					DM	The range of voxel intensities (Wavelet LLH stats range; c-index range: 0.67)	
					LRR	None	
					LR	2 statistic features and 3 texture features	
					Labor recurrence	1 statistic feature and 2 texture features	
	SBRT	I-IIA	112	20.8 months	DM (FB vs AIP)	AIP: 7 radiomics features describe shape and heterogeneity (c-index range: 0.638-0.676)	Huynh *et al* [28]
					LRR (FB vs AIP)	None	
	SBRT	I-IIA	92	39.2 months	OS	ECOG performance status, pleural retraction, F2 (short axis × longest diameter, F186 (Hist-Energy-L1) (HR: 2.78, 0.27, 1.72, 1.27; 95% CI: 1.37-5.65, 0.08-0.92, 1.21-2.44, 1.00-1.61);	Li *et al*[73]
					RFS	Vessel attachment, F2 (HR: 2.13, 1.69; 95% CI: 1.24-3.64, 1.33-2.15)	
					LRFS	ECOG performance status, F2 (HR: 2.01, 1.67; 95% CI: 1.12-3.60, 1.29-2.18)	
	CRT	III	91	59 months	OS	Combine texture features and conventional prognostic factors ($P = .046$)	Fried *et al*[74]
					DM	Combine texture features and conventional prognostic factors ($P = .005$)	
					LRC	Combine texture features and conventional prognostic factors ($P = .01$)	
	CRT	II-III	182(98+84)	23.7 months(OS:24.7 months;DM: 13.4 months)	DM	35 Radiomics features (c-index >0.60, FDR<5%), tumor volume (c-index: 0.55; *P*: 2.77×10^{-5})	Coroller *et al* [75]
					OS	12 features	
	CRT	II-III	127	41.8 months	Pathological response	GRD: 7 radiomics features (AUC: 0.61–0.66, $P < .05$); pCR: 1 radiomics features, rounder shape, heterogeneous texture (AUC: 0.63, 0.63, 0.61; $P = .01, .009, .03$)	Coroller *et al*[8]
	CRT	II, III	85	40.2 months	Pathological response	pCR: 3 radiomics features (AUC: 0.67, $P < .05$); GRD: 2 radiomics features (AUC: 0.72-0.75, $P < .05$)	Coroller *et al*[7]
	CRT (451), RT (196)	I-IIIB	647 (422 + 225)	750 days	OS	238 features (54%) of 440 features quantifying image shape, intensity, and texture (FDR: 10%)	Aerts *et al*[45]
	RT	I-IV	288 (132 + 62 + 94)	15.0 months, 15.0 months, 25.5 months	OS	13.3% (149/1119) radiomics features: $R^2 > 0.85$; 4 radiomics features in data set 1, 2, 3: c-index: 0.69, 0.43, 0.45; 95% CI: 0.63-0.75, 0.34-0.51, 0.38-0.52; *P*: 4.0×10^{-10}, 0.08, 0.16	van Timmeren *et al*[76]
	TKI	I-IV	152 (80 + 72)	9.5 months, 10.2 months	PFS	2 texture features (HR: 2.13, 2.43; 95% CI: 1.33-3.40, 1.46-4.05, $P = .010, .005$)	Song *et al*[77]

Abbreviations: AIP, average intensity projection; AUC, area under the receiver operating characteristic curve; AUC-CSH, area under the curve of the cumulative SUV-volume histogram; c-index, concordance index; 95% CI, 95% confidence interval; COV, coefficient of variation; CRT, chemoradiotherapy; CT, computed tomography; DFS, disease-free survival; DM, distant metastases; DMFS, distant metastasis–free survival; DSS, disease-specific survival; ECOG, Eastern Cooperative Oncology Group; FB, free breathing; FDR, false discovery rate; GRD, gross residual disease; HR, hazard ratio; IVH, intensity–volume histogram; LoG, Laplacian transform of Gaussisn filter; LR, local recurrence; LRC, local-regional control; LRFS, locoregional recurrence-free survival; LRR, loco-regional recurrence; OS, overall survival; pCR, pathologic complete remission; PET, positron emission tomography; PFS, progression-free survival; R^2, coefficient of determination; RECIST, Response Evaluation Criteria in Solid Tumors; RFS, recurrence-free survival; *r*s, Spearman correlation; RT, radiotherapy; SBRT, stereotactic body radiotherapy; SUV, standardized uptake value; SUV_{max}, maximum standardized uptake value; TKI, tyrosine kinase inhibitors.

Table 3. Delta-Radiomics in Response Assessment and Treatment Outcome Prediction.

Studied Images	Treatment	Stage	N	Early Prediction Time Point	End Point	Image Parameter Related to Results (*P* Value, c-index, AUC, HR, etc)	Reference
PET only	SBRT	I	128 (68 + 60)	6.1 months to 12 months	LR	Median SUV_{max} of 6.1-12 months and 12.1-24 months ($P < .001$)	Zhang et al 2012[53]
	SBRT	I	132	12 weeks	2-year LC	SUV_{max} 5.0 cutoff (SHR: 7.3; 95% CI: 1.4-38.5; *P*: .019)	Bollineni et al 2012[56]
					DSS	SUV_{max} 5.0 cutoff (SHR: 2.2; 95% CI: 0.8-6.3; $P = .113$)	
					OS	SUV_{max} 5.0 cutoff (SHR:1.6; 95% CI: 0.7-3.7; $P = .268$)	
	SBRT	I	29	1 year	LR	$SUV_{mean} > 3.44$, 5.48, reduction in SUV_{mean} or $SUV_{max} < 43\%$, 52% ($P = .001$, .009, .03, .025)	Essler et al[78]
					DSS	$SUV_{mean} > 2.81$, 3.45, reduction in SUV_{mean} or $SUV_{max} < 32\%$, 52% ($P = .023$, .007, .015,.013)	
	CRT	III	58	28 ± 3 days	RECIST–response	Pretreatment COV, MTV, contrast (AUC: 0.781, 0.686, 0.804), and Δ radiomics	Dong et al.[79]
					PFS	Δ contrast (HR: 0.476; $P = .021$)	
					OS	Δ contrast (HR: 0.519; $P = .015$)	
	(C)RT	IIIA-IV	54	2 weeks	OS	A Δ radiomics predictive model (internal and external: c-index: 0.64, 0.61; $P < .01$, .05)	Carvalho et al [80]
	Chemo-erlotinib	IIIB, IV	47	6 weeks	RECIST–response	First-order SD, uniformity, Δ entropy ($P = .01$,.001, .001,.01).	Cook et al.[12]
					OS	Contrast, Δ entropy ($P = .002$, .03)	
PET and CT	SBRT	TI-T4	257	1 year	LR	LR vs non-LR: median SUV_{maxs} (early image: 5.0, 1.8; late image: 6.3, 1.7; RI: 0.20, 0.00; $P < .05$)	Takeda [81]
CT only	SBRT	I	22	9 months	Distinguish RILI from recurrence	Consolidative changes ($P = .046$) and SD of HU ($P = .0078$)	Mattonen et al.[15]
	SBRT	I	22	<5 months	Recurrence	First-order texture, entropy, and energy (AUC: 0.79-0.81)	Mattonen *et al.*[82]
	SBRT	I-II	45	<6 months	Recurrence (physician vs radiomics)	Radiomic signature contains 5 image features can detect recurrence earlier than physician (AUC: 0.85)	Mattonen et al.[83]
	SBRT	I	14	3 months	Distinguish RILI severity levels	The GLCM features ($P = .012$-.262; AUC: 0.643-0.750); the first-order features ($P = .100$-.990; AUC: 0.543-0.661)	Moran et al [84]
	CRT	II-IV	107	DM: <3 months; OS: <1 month; LR: <2 months	DM	Clinical factors alone, combined with pretreatment features (c-index: 0.539, 0.632; $P = .38$, .00156)	Fave et al.[85]
					OS	Clinical factors, pretreatment features and Δ radiomics features (c-index: 0.675; $P = 1.3\times10^{-5}$)	
					LR	Clinical factors, pretreatment features, and Δ radiomics features (c-index: 0.558; $P = .0269$)	
	RT	I-III	14	<2 weeks	Treatment response	The mean HU reductions in GTV associate with the accumulated GTV dose ($R^2 > 0.99$)	Paul et al[87]
					OS	Higher mean HU reductions in GTV ($P = .038$)	
	Gefitinib	Early stage	47	3 weeks	EGFR mutation status	Law's, energy, Δ volume, Δ maximum diameter, Δ Gabor energy (AUC: 0.67, 0.91, 0.78, 0.74; $P = .03$, 10^{-25}, 10^{-5}, .0003)	Aerts, 2016[6]
	TKI	IIIA	23	4-6 weeks	Pathologic response	Intensity variability and size zone variability	Chong[86]
	CRT		28			Volume, mass, kurtosis, and skewness	

Abbreviations: AUC, areas under the receiver operating characteristic curve; c-index, concordance index; 95% CI, 95% confidence interval; COV, coefficient of variation; CRT, chemoradiotherapy; CT, computed tomography; DM, distant metastases; DSS, disease-specific survival; EGFR, epidermal growth factor receptor; GLCM, gray-level cooccurrence matrix; GTV, gross tumor volume; HR, hazard ratio; HU, Hounsfield unit; Law's, Law's texture measures; LC, local control; LR, local recurrence; MTV, metabolic tumor volume; OS, overall survival; PET, positron emission tomography; PFS, progression-free survival; R^2, coefficient of determination; RECIST, Response Evaluation Criteria in Solid Tumors; RI, retention index; RILI, radiation-induced lung injury; RT, radiotherapy; SBRT, stereotactic body radiotherapy; SD, standard deviation; SHR, adjusted subhazard ratio; SUV_{max}, maximum standardized uptake value; SUV_{mean}, average standardized uptake value; TKI, tyrosine kinase inhibitors; Δ, delta.

texture feature and changes in volume, maximum diameter, and a filter-based feature were proved significant.

The RECIST response has its limitation in diversified clinical applications.[88] Radiomic features such as texture features and volume changes have the potential to better predict tumor responses and thus may be considered as new tumor response phenotypes that provide diversified information in the future.

Survival Analysis

Studies focusing on survival analysis include OS, progression-free survival (PFS), locoregional recurrence-free survival (LRFS), distant metastasis–free survival (DMFS), disease-free survival (DFS), disease-specific survival (DSS), and so on.

Positron emission tomography images. For predicting survivals based on PET images, the best features ever found are: the high-order contrast for OS ($P = .002$),[12] AUC of the cumulative SUV-volume histogram (AUC-CSH) for PFS, LRFS, and DMFS ($P < .001, = .002, = .003$),[54] and mean SUV (SUV_{mean}) greater than 3.45 for DSS ($P = .007$).[78] Kang *et al*[54] revealed that maximum SUV (SUV_{max}) and AUC-CSH reflecting tumor heterogeneity were significant prognostic factors for PFS, while AUC-CSH were for LRFS and DMFS.[54] Carvalho *et al*[55] showed that tumor's relative volume containing >80% SUV significantly correlates with OS, and a larger tumor's relative volume above a higher SUV can lead to better prognosis. Furthermore, the texture feature SumMean for OS by Ohri *et al*[71] and textural feature dissimilarity for DSS and DFS by Lovinfosse *et al*[70] are shown to be more powerful independent predictors compared to metabolic metrics. Aside from these features, conventional clinical factors, such as gender, age, histology, stage, and so on, have also been discussed by Lovinfosse *et al*[70] and Fried *et al*[72] The latter showed that the combination of quantitative features with conventional clinical features can improve OS risk stratification compared with conventional clinical features alone.[72] In addition, delta-radiomics features of fludeoxyglucose-PET are correlated with OS in patients with NSCLC. Carvalho *et al*[80] validated the predictive capacity in delta-radiomics features (volume, texture features, and intensity–volume histogram [IVH]) and demonstrated their correlations with OS.

Computed tomography images. Radiomics features in CT images can predict OS better than PET images. A radiomics model based on pretreatment CT and recalibrated cone beam CT images in van Timmeren *et al* study (concordance index = 0.69, $P = 4.0 \times 10^{-10}$) and a combination model of pretreatment features and delta radiomics features in Fave *et al*'s study (c-index = 0.675; $P = 1.3 \times 10^{-5}$) are significant predictors for OS.[74,85,89] Overall, in survival studies based on CT images, those radiomics features quantifying shapes, intensity, and texture, conventional features (such as Eastern Cooperative Oncology Group performance status, pleural retraction, and diameter), and delta-radiomics features are predictive, and when they are combined with clinical factors, the predictive capacity can be significantly improved.[32,45,74,85]

Recurrence Prediction After Treatment

Positron emission tomography images. For recurrence prediction after treatment based on PET images, SUV metrics and texture features were both discussed in recent literature. Takeda *et al*,[81] Essler *et al*[78] and Zhang *et al*[53] assessed local recurrence (LR) in patients with NSCLC after stereotactic body radiotherapy (SBRT) by PET images and showed SUV metrics as strong LR predictors, that is, dual-time-point SUV_{max} or SUV_{maxs} in the study by Takeda *et al*,[81] SUV_{mean} >3.44, SUV_{max} > 5.48, and their reduction in the study by Essler *et al*,[78] and the cutoff SUV_{max} of 5 with 100% sensitivity and 91% specificity in the study by Zhang *et al*[53] However, SUV metrics are reported less correlated when compared with other features, such as IVH, texture features, and so on. Pyka *et al*[69] assessed the relationship of texture features with LR in PET images for patients with NSCLC after radiotherapy and reported that several texture features such as entropy (AUC = 0.872) and correlation (AUC = 0.816) had higher AUC values than SUV metrics in receiver operating characteristic analysis.

Computed tomography images. Computed tomography–based radiomics features exhibited lack of prognostic power for locoregional recurrence (LRR) in many studies,[28,32] while 5 pretreatment statistic and texture features in the study by Huynh *et al* and end-treatment texture-strength feature in the study by Fave *et al* are prognostic for LR, and 3 pretreatment statistic and texture features in Huynh *et al* are prognostic for lobar recurrence.[28,32,81,85] Although CT-based radiomic features are limited in their ability to predict recurrence compared to other outcomes, they have the ability to distinguish tumor recurrences on follow-up CT images earlier than human eyes. Mattonen *et al*[83] compared the predictive ability between doctors and radiomic features. Although physicians' average predictive accuracy rate was 83% for the average prediction period of 15.5 months, they misdiagnosed at an average error rate of 35%, a false-positive rate (FPR) of 1%, and a false-negative rate (FNR) of 99% when the follow-up period was shortened to 6 months after radiotherapy. In contrast, the studied five radiomics features can accurately determine the recurrence rate with AUC value of 0.85, classification error rate of 24%, FPR of 24%, FNR of 23% at 6 months.

These recurrence studies show that PET features own higher predictive abilities and accuracy in tumor recurrence than CT features.[81] Vaidya *et al*[52] also studied the capacity of combined PET and CT image features, such as SUV or HU, IVH, and texture features, for LRR prediction in patients with NSCLC after radiotherapy. It was found that a 2-parameter model of PET and CT features had higher prediction accuracy for LRR than PET or CT features alone. Thus, multimodality radiomics features are superior in predicting tumor recurrence.

Distinguishing RILI

Computed tomography images. Radiomic features from CT images also demonstrated high potentials in distinguishing tumor RILI from recurrence[15] and RILI severity levels.[84] Mattonen *et al*[15] showed that compared with RILI, tumor recurrence showed higher HU,and higher SD in ground-glass opacity (GGO) texture measure. When comparing conventional features (RECIST and volume) and quantitative changes in CT number (HU) with GGO textural feature, results showed the predictive time points to distinguish RILI and recurrence in advance is 9 months post-SBRT and 15 months post-SBRT, respectively. Another publication by the same group[82] described that GGO textural analysis has potential to predict recurrence within 5 months post-SBRT. Similar texture analysis methods were adopted by Moran *et al*,[84] where first-order and gray-level co-occurrence matrix texture features were extracted to distinguish RILI severity levels: none/mild, moderate, and severe. Gray-level co-occurrence matrix texture features ($P = .012$-$.262$; AUC = 0.643-0.750) have been reported to provide a better performance than first-order features ($P = .100$-$.990$; AUC = 0.543-0.661). Cunliffe *et al*[90] also combined radiomic features with radiation dose and demonstrated that radiomics can provide a quantitative, personalized measurement of radiation dose tolerance for individual patients, which can be used to determine the possibility of radiation-induced pneumonitis and monitor its progression.

Distant Metastases Evaluation

Positron emission tomography images. For DM evaluation in PET images radiomics studies, the optimal prognostic model including two quantitative image features of intratumoral heterogeneity and average of the voxel with SUV_{max} of the tumor region (SUV_{peak}; c-index = 0.71) were shown to be able to predict and categorize patients into low- and high-risk groups. Furthermore, when tumors' histologic types were combined, the prognostic power of the model was significantly improved.[57] Interestingly, it was presented that neither PET metrics nor texture features were related to DM in the study by Pyka *et al.*[69]

Computed tomography images. For DM evaluation in CT images radiomics studies, one pretreatment feature describing the range of voxel intensities (Wavelet LLH stats range; c-index = 0.67) and seven pretreatment average intensity projection CT radiomics features describing shape and heterogeneity (c-index = 0.638-0.676) in the study by Huynh *et al* perform well.[28,32] Also, Coroller *et al* found strong prognostic powers in radiomic features, among which Laplacian transform of Gaussian (LoG) filter features showed the best performance (c-index = 0.61, $P < .001$).[75] Besides, combining pretreatment texture features with clinical prognostic factors can significantly improve their predictive abilities.[74,85]

It is worth noting that only three studies[57,72,80] provided feature validation. Therefore, even though results were shown promising, lack of feature validation may lead to false positive and might shadow doubts in the subsequent correlation studies.

Current Research Challenges and Prospects

Published studies show promising results in NSCLC treatments, yet there are still major challenges and limitations to resolve before they can be translated into reliable clinical application. A number of experimental clinical studies have found that current restrictions of radiomics in its therapeutic application are mainly subjected to (1) image standardization,[29,91] (2) image registration,[92-94] and (3) data sharing.[5] The on-going research activities focusing on tackling these limitations are elaborated subsequently.

Standardization of Images

Variations in scanning devices, acquisition modes, reconstruction parameters, and scanning protocols may impact subsequent feature analysis as mentioned in "The Workflow of radiomics". A study on feature stability in CT perfusion maps showed that none of radiomics parameters were stable without standardization, especially for voxel size, temporal resolution, HU threshold, image discretization, and so on.[91] There are two ways to solve the problem. One is to develop software to calibrate existing image data for retrospective analysis. But the excepted standardization is still difficult to achieve due to the vast variations in calibration algorithms.[95] The other method is to design prospective trials where all enrolled patients receive standardized image scans. In addition, there are national image centers that are currently being planned or constructed, where images can be obtained within one entity in order to fundamentally resolve the image nonstandardizing issue.[19,95]

Image Registration

Image registrations, including both rigid and deformable, are commonly used in the course of radiotherapy treatment of NSCLC.[92] The concept of delta-radiomics demands high accuracy in image registration when comparing pretreatment images with posttreatment images and images during treatment. Image registration can be achieved by manual, automatic, or the combination of both.[96,97] At present, the commonly used automatic registration algorithms include image intensity-based method, and structure-based method.[94,97] Although the impact of image registration on texture features and change assessment of serial thoracic CT scans have been studied,[93,98,99] it still remains unclear how image registration accuracy can affect radiomics results and which method would work the best for delta-radiomics for NSCLC. Future study areas can be large-scale prospective clinical trials with the application of delta-radiomics.

Data Storage and Data Sharing

Radiomics study relies heavily on the statistical analysis. Sample size is a critical defect in current research. As shown in Tables 2 and 3, most studies cover limited number of patients, with one exception that contains a large patient sample of 647.[45] Small sample size poses an obstacle for obtaining high correlations between radiomics features and treatment outcomes with high confidence interval. Big data are the premise of using technology to mine the radiomics features and ensure statistical significance in data analysis. The establishment of patient database can strengthen standardized management and improve utilization efficiency. The high-number and high-quality database is the basis for radiomics study, in order to effectively predict outcome. Image data storage and standardization require joint efforts by companies and/or institutions. Institutions such as Cancer Learning Intelligence Network for Quality and Flatiron Health are working on data aggregating.[100]

Additionally, the robustness and stability of the discovered features need improvement before they are applied to clinical treatment assistance in NSCLC, so validation and further clinical practice are essential. Future research can also be prospectively designing clinical trials with the focus on implementing discovered experimental features with high statistical significance.

Future Developments in Radiomics for Managing NSCLC

With artificial intelligence being adopted to medical field and the optimization of machine learning algorithm, limitations in image preprocessing, that is, ROI segmentation, feature extraction, and feature selection/classification, may be greatly improved or even eliminated in a foreseeable future.

The applications are still not adequate to provide satisfactory optimized summary information to direct clinicians in medical and radiation oncology on how to further manage their patients, and more "standardized" data are needed from institutions to create these programs. Standardizing is required not only for image acquisition but also for all the steps in the radiomics workflow as mentioned in "The Workflow of radiomics", as well as all personnel involved, including those in medical and radiation oncology professions. There is a cultural change underway to capture these big data in pursuit of personalized medicine for patients with NSCLC, and many efforts are underway by American Society for Radiation Oncology, the American Association of Physicists in Medicine, and American Society of Clinical Oncology to name a few.[91]

The Cancer Imaging Archive, a National Cancer Institute–funded information repository that aggregates images (radiology, pathology), radiation therapy information objects, annotations, clinical trial data, and information derived from quantitative image analysis to support big data analytics, is an example of a comprehensive approach to acquiring, archiving, and extracting data that will be useful for the predictive models that are needed for radiomics to be fully utilized and a great value to clinicians and their patients.

Conclusion

Radiomics process to assess tumor response and predict recurrence, survival, DM, and RILI in NSCLC mainly includes imaging acquisition/reconstruction, ROI definition/segmentation, image feature extraction, and image feature selection and classification. Features quantifying target shape, size, volume, intensity, texture, and so on, are able to predict outcome and assess response. Among them, texture features outperform the others for predicting tumor response, survival, recurrence, DM, and RILI in PET/CT images and CT images. Delta-radiomics, which compares the changes within those features extracted from pretreatment images and follow-up images during and/or after the treatment, are able to identify signs of recurrence, metastases, or death early. Image standardization, image registration, and data sharing are main challenges and limitations for the clinical applications of radiomics tools. Additionally, validation and clinical practice are also essential before radiomics applied to clinical treatment guidance for NSCLC.

Authors' Note

Liting Shi and Yaoyao He contributed equally to the work.

Acknowledgments

Authors would like to thank Dr. T Li for her contribution in proofreading a couple paragraphs.

Declaration of Conflicting Interests

The author(s) declared no potential conflicts of interest with respect to the research, authorship, and/or publication of this article.

Funding

The author(s) disclosed receipt of the following financial support for the research, authorship, and/or publication of this article: This study received fundings from the China National Key Research and Development Program (2016YFC0103400) and Shandong Province Key Research and Development Program (2017GSF218075). Jianfeng Qiu is supported by the Taishan Scholars Program of Shandong Province.

ORCID iD

Yi Rong, PhD http://orcid.org/0000-0002-2620-1893

References

1. Stewart B, Wild CP. (eds), International Agency for Research on Cancer, WHO. World Cancer Report 2014. *Health*. 2014 pp. 350-361. ISBN 978-92-832-0443-5. http://www.thehealthwell.info/node/725845
2. Scrivener M, de Jong EE, van Timmeren JE, Pieters T, Ghaye B, Geets X. Radiomics applied to lung cancer: a review. *Transl Cancer Res*. 2016;5(4):398-409.
3. Histed SN, Lindenberg ML, Mena E, Turkbey B, Choyke PL, Kurdziel KA. Review of functional/anatomical imaging in oncology. *Nucl Med Commun*. 2012;33(4):349-361.

4. Lambin P, Rios-Velazquez E, Leijenaar R, et al. Radiomics: extracting more information from medical images using advanced feature analysis. *Eur J Cancer*. 2012;48(4):441-446.
5. Kumar V, Gu Y, Basu S, et al. Radiomics: the process and the challenges. *Magn Reson Imaging*. 2012;30(9):1234-1248.
6. Aerts HJ, Grossmann P, Tan Y, et al. Defining a radiomic response phenotype: a pilot study using targeted therapy in NSCLC. *Sci Rep*. 2016;6(1):33860.
7. Coroller TP, Agrawal V, Huynh E, et al. Radiomic-based pathological response prediction from primary tumors and lymph nodes in NSCLC. *J Thorac Oncol* 2017;12(3):467-476.
8. Coroller TP, Agrawal V, Narayan V, et al. Radiomic phenotype features predict pathological response in non-small cell lung cancer. *Radiother Oncol*. 2016;119(3):480-486.
9. Mattonen SA. Radiomics for response assessment after stereotactic radiotherapy for lung cancer. *Electro Thesis Dissertat Reposit*. 2016. Paper 3926.
10. Mattonen SA, Huang K, Ward AD, Senan S, Palma DA. New techniques for assessing response after hypofractionated radiotherapy for lung cancer. *J Thorac Dis*. 2014;6(4):375-386.
11. Apostolova I, Rogasch JM, Buchert R, et al. Quantitative assessment of the asphericity of pretherapeutic FDG uptake as an independent predictor of outcome in NSCLC. *BMC Cancer*. 2014; 14(1):896.
12. Cook GJ, O'Brien ME, Siddique M, et al. Non-small cell lung cancer treated with erlotinib: heterogeneity of (18)F-FDG uptake at PET-association with treatment response and prognosis. *Radiology*. 2015;276(3):883-893.
13. Cook GJ, Yip C, Siddique M, et al. Are pretreatment 18F-FDG PET tumor textural features in non-small cell lung cancer associated with response and survival after chemoradiotherapy? *J Nucl Med*. 2013;54(1):19-26.
14. Scheckenbach K, Colter L, Wagenmann M. Radiomics in head and neck cancer: extracting valuable information from data beyond recognition. *ORL J Otorhinolaryngol Relat Spec*. 2017; 79(1-2):65-71.
15. Mattonen SA, Palma DA, Haasbeek CJ, Senan S, Ward AD. Distinguishing radiation fibrosis from tumour recurrence after stereotactic ablative radiotherapy (SABR) for lung cancer: a quantitative analysis of CT density changes. *Acta oncologica*. 2013;52(5):910-918.
16. Scalco E, Rizzo G. Texture analysis of medical images for radiotherapy applications. *Br J Radiol*. 2017;90(1070):20160642.
17. Parekh V, Jacobs MA. Radiomics: a new application from established techniques. *Expert Rev Precis Med Drug Dev*. 2016;1(2): 207-226.
18. Lee G, Lee HY, Park H, et al. Radiomics and its emerging role in lung cancer research, imaging biomarkers and clinical management: state of the art. *Eur J Radiol*. 2017;86:297-307.
19. Gillies RJ, Kinahan PE, Hedvig H. Radiomics: images are more than pictures, they are data. *Radiology*. 2015;278(2):563-577.
20. Limkin EJ, Sun R, Dercle L, et al. Promises and challenges for the implementation of computational medical imaging (radiomics) in oncology. *Ann Oncol*. 2017;28(6):1191-1206.
21. Yip SS, Aerts HJ. Applications and limitations of radiomics. *Phys Med Biol*. 2016;61(13): R150-R166.
22. Lu W, Chen W. Positron emission tomography/computerized tomography for tumor response assessment-a review of clinical practices and radiomics studies. *Transl Cancer Res*. 2016;5(4): 364-370.
23. Alobaidli S, McQuaid S, South C, Prakash V, Evans P, Nisbet A. The role of texture analysis in imaging as an outcome predictor and potential tool in radiotherapy treatment planning. *Br J Radiol*. 2014;87(1042):20140369.
24. Sollini M, Cozzi L, Antunovic L, Chiti A, Kirienko M. PET Radiomics in NSCLC: state of the art and a proposal for harmonization of methodology. *Sci Rep*. 2017;7(1):358.
25. Emaminejad N, Qian W, Guan Y, et al. Fusion of quantitative image and genomic biomarkers to improve prognosis assessment of early stage lung cancer patients. *IEEE Trans Biomed Eng*. 2016;63(5):1034-1043.
26. He L, Huang Y, Ma Z, Liang C, Liang C, Liu Z. Effects of contrast-enhancement, reconstruction slice thickness and convolution kernel on the diagnostic performance of radiomics signature in solitary pulmonary nodule. *Sci Rep*. 2016;6:34921.
27. Grootjans W, Tixier F, van der Vos CS, et al. The impact of optimal respiratory gating and image noise on evaluation of intratumor heterogeneity on 18F-FDG PET imaging of lung cancer. *J Nucl Med*. 2016;57(11):1692-1698.
28. Huynh E, Coroller TP, Narayan V, et al. Associations of radiomic data extracted from static and respiratory-gated CT scans with disease recurrence in lung cancer patients treated with SBRT. *PloS One*. 2017;12(1): e0169172.
29. Galavis PE, Hollensen C, Jallow N, Paliwal B, Jeraj R. Variability of textural features in FDG PET images due to different acquisition modes and reconstruction parameters. *Acta Oncol*. 2010; 49(7):1012-1016.
30. Mackin D, Fave X, Zhang L, et al. Measuring computed tomography scanner variability of radiomics features. *Invest Radiol*. 2015;50(11):757-765.
31. Mattonen SA, Tetar S, Palma DA, Louie AV, Senan S, Ward AD. Imaging texture analysis for automated prediction of lung cancer recurrence after stereotactic radiotherapy. *J Med Imag*. 2015;2(4): 041010.
32. Huynh E, Coroller TP, Narayan V, et al. CT-based radiomic analysis of stereotactic body radiation therapy patients with lung cancer. *Radiother Oncol*. 2016;120(2):258-266.
33. Louie AV, Rodrigues G, Olsthoorn J, et al. Inter-observer and intra-observer reliability for lung cancer target volume delineation in the 4D-CT era. *Radiother Oncol*. 2010;95(2):166-171.
34. Cao Y. The promise of dynamic contrast-enhanced imaging in radiation therapy. *Semin Radiat Oncol*. 2011;21(2):147-156.
35. Sensakovic WF, Armato SG, 3rd, Straus C, et al. Computerized segmentation and measurement of malignant pleural mesothelioma. *Med Phys*. 2011;38(1):238-244.
36. Balagurunathan Y, Gu Y, Wang H, et al. Reproducibility and prognosis of quantitative features extracted from CT images. *Transl Oncol*. 2014;7(1):72-87.
37. Leijenaar RT, Carvalho S, Velazquez ER, et al. Stability of FDG-PET radiomics features: an integrated analysis of test-retest and inter-observer variability. *Acta Oncol*. 2013;52(7):1391-1397.

38. van Velden FH, Kramer GM, Frings V, et al. Repeatability of radiomic features in non-small-cell lung cancer [(18)F]FDG-PET/CT studies: impact of reconstruction and delineation. *Mol Imaging Biol*. 2016;18(5):788-795.
39. Parmar C, Rios Velazquez E, Leijenaar R, et al. Robust radiomics feature quantification using semiautomatic volumetric segmentation. *PloS one*. 2014;9(7): e102107.
40. Rios Velazquez E, Aerts HJ, Gu Y, et al. A semiautomatic CT-based ensemble segmentation of lung tumors: comparison with oncologists' delineations and with the surgical specimen. *Radiother Oncol*. 2012;105(2):167-173.
41. Gu Y, Kumar V, Hall LO, et al. Automated delineation of lung tumors from CT images using a single click ensemble segmentation approach. *Pattern Recognit*. 2013;46(3):692-702.
42. Bartko JJ. The intraclass correlation coefficient as a measure of reliability. *Psychol Rep*. 1966;19(1):3-11.
43. Doumou G, Siddique M, Tsoumpas C, Goh V, Cook GJ. The precision of textural analysis in (18)F-FDG-PET scans of oesophageal cancer. *Eur Radiol*. 2015;25(9):2805-2812.
44. Kalpathy-Cramer J, Mamomov A, Zhao B, et al. Radiomics of lung nodules: a multi-institutional study of robustness and agreement of quantitative imaging features. *Tomography*. 2016;2(4):430-437.
45. Aerts HJ, Velazquez ER, Leijenaar RT, et al. Decoding tumour phenotype by noninvasive imaging using a quantitative radiomics approach. *Nat Commun*. 2014;5:4006.
46. Liu Y, Balagurunathan Y, Atwater T, et al. Radiological image traits predictive of cancer status in pulmonary nodules. *Clin Cancer Res*. 2017;23(6):1442-1449.
47. Prosch H. Implementation of lung cancer screening: promises and hurdles. *Transl Lung Cancer Res*. 2014;3(5):286-290.
48. Hu H, Wang Q, Tang H, Xiong L, Lin Q. Multi-slice computed tomography characteristics of solitary pulmonary ground-glass nodules: differences between malignant and benign. *Thorac Cancer*. 2016;7(1):80-87.
49. Bayanati H, Thornhill ET, Souza CA, et al. Quantitative CT texture and shape analysis: can it differentiate benign and malignant mediastinal lymph nodes in patients with primary lung cancer? *Eur Radiol*. 2015;25(2):480-487.
50. Andersen MB, Harders SW, Ganeshan B, Thygesen J, Torp Madsen HH, Rasmussen F. CT texture analysis can help differentiate between malignant and benign lymph nodes in the mediastinum in patients suspected for lung cancer. *Acta Radiol*. 2016;57(6): 669-676.
51. Vallières M, Freeman CR, Skamene SR, Naqa IE. A radiomics model from joint FDG-PET and MRI texture features for the prediction of lung metastases in soft-tissue sarcomas of the extremities. *Phys Med Biol*. 2015;60(14):5471-5496.
52. Vaidya M, Creach KM, Frye J, Dehdashti F, Bradley JD, El Naqa I. Combined PET/CT image characteristics for radiotherapy tumor response in lung cancer. *Radiother Oncol*. 2012;102(2):239-245.
53. Zhang X, Liu H, Balter P, et al. Positron emission tomography for assessing local failure after stereotactic body radiotherapy for non-small-cell lung cancer. *Int J Radiat Oncol Biol Phys*. 2012; 83(5):1558-1565.
54. Kang SR, Song HC, Byun BH, et al. Intratumoral metabolic heterogeneity for prediction of disease progression after concurrent chemoradiotherapy in patients with inoperable stage III non-small-cell lung cancer. *Nucl Med Mol Imaging*. 2014;48(1):16-25.
55. Carvalho S, Leijenaar RT, Velazquez ER, et al. Prognostic value of metabolic metrics extracted from baseline positron emission tomography images in non-small cell lung cancer. *Acta Oncol*. 2013;52(7):1398-1404.
56. Bollineni VR, Widder J, Pruim J, Langendijk JA, Wiegman EM. Residual 18 F-FDG-PET uptake 12 weeks after stereotactic ablative radiotherapy for stage I non-small-cell lung cancer predicts local control. *Int J Radiat Oncol Biol Phys*. 2012;83(4): e551-e555.
57. Wu J, Aguilera T, Shultz D, et al. Early-stage non-small cell lung cancer: quantitative imaging characteristics of (18)F fluorodeoxyglucose PET/CT allow prediction of distant metastasis. *Radiology*. 2016;281(1):270-278.
58. Zhang Y, Oikonomou A, Wong A, Haider MA, Khalvati F. Radiomics-based prognosis analysis for non-small cell lung cancer. *Sci Rep*. 2017;7:46349.
59. Parmar C, Grossmann P, Rietveld D, Rietbergen MM, Lambin P, Aerts HJ. Radiomic machine-learning classifiers for prognostic biomarkers of head and neck cancer. *Front Oncol*. 2015;5:272.
60. Saeys Y, Inza I, Larranaga P. A review of feature selection techniques in bioinformatics. *Bioinformatics*. 2007;23(19): 2507-2517.
61. Dy JG, Brodley CE. Feature selection for unsupervised learning. *J Mach Learn Res*. 2004;5:845-889.
62. Parmar C, Grossmann P, Bussink J, Lambin P, Aerts HJ. Machine learning methods for quantitative radiomic biomarkers. *Sci Rep*. 2015;5:13087.
63. Guyon I, Elisseeff A. An introduction to variable and feature selection. *J Mach Learn Res*. 2003;3(Mar):1157-1182.
64. Madero Orozco H, Vergara Villegas OO, Cruz Sanchez VG, Ochoa Dominguez Hde J, Nandayapa Alfaro Mde J. Automated system for lung nodules classification based on wavelet feature descriptor and support vector machine. *Biomed Eng Online*. 2015; 14:9.
65. Keshani M, Azimifar Z, Tajeripour F, Boostani R. Lung nodule segmentation and recognition using SVM classifier and active contour modeling: a complete intelligent system. *Comput Biol Med*. 2013;43(4):287-300.
66. Kuruvilla J, Gunavathi K. Lung cancer classification using neural networks for CT images. *Comput Methods Programs Biomed*. 2014;113(1):202-209.
67. Kourou K, Exarchos TP, Exarchos KP, Karamouzis MV, Fotiadis DI. Machine learning applications in cancer prognosis and prediction. *Comput Struct Biotechnol J*. 2015;13:8-17.
68. Xiao Y, Wu J, Lin Z, Zhao X. A deep learning-based multi-model ensemble method for cancer prediction. *Comput Methods Programs Biomed*. 2018;153:1-9.
69. Pyka T, Bundschuh RA, Andratschke N, et al. Textural features in pre-treatment [F18]-FDG-PET/CT are correlated with risk of local recurrence and disease-specific survival in early stage NSCLC patients receiving primary stereotactic radiation therapy. *Radiat Oncol*. 2015;10(1):100.
70. Lovinfosse P, Janvary ZL, Coucke P, et al. FDG PET/CT texture analysis for predicting the outcome of lung cancer treated by

stereotactic body radiation therapy. *Eur J Nucl Med Mol Imaging*. 2016;43(8):1453-1460.
71. Ohri N, Duan F, Snyder BS, et al. Pretreatment 18F-FDG PET textural features in locally advanced non-small cell lung cancer: secondary analysis of ACRIN 6668/RTOG 0235. *J Nucl Med*. 2016;57(6):842-848.
72. Fried DV, Mawlawi O, Zhang L, et al. Stage III non-small cell lung cancer: prognostic value of FDG PET quantitative imaging features combined with clinical prognostic factors. *Radiology*. 2016;278(1):214-222.
73. Li Q, Kim J, Balagurunathan Y, et al. Imaging features from pretreatment CT scans are associated with clinical outcomes in nonsmall-cell lung cancer patients treated with stereotactic body radiotherapy. *Med Phys*. 2017;44(8):4341-4349.
74. Fried DV, Tucker SL, Zhou S, et al. Prognostic value and reproducibility of pretreatment CT texture features in stage III non-small cell lung cancer. *Int J Radiat Oncol Biol Phys*. 2014; 90(4):834-842.
75. Coroller TP, Grossmann P, Hou Y, et al. CT-based radiomic signature predicts distant metastasis in lung adenocarcinoma. *Radiother Oncol*. 2015;114(3):345-350.
76. van Timmeren JE, Leijenaar RTH, van Elmpt W, et al. Survival prediction of non-small cell lung cancer patients using radiomics analyses of cone-beam CT images. *Radiother Oncol*. 2017; 123(3):363-369.
77. Song J, Dong D, Huang Y, Zang Y, Liu Z, Tian J. Association between tumor heterogeneity and progression-free survival in non-small cell lung cancer patients with EGFR mutations undergoing tyrosine kinase inhibitors therapy. *Conf Proc IEEE Eng Med Biol Soc*. 2016:1268-1271.
78. Essler M, Wantke J, Mayer B, et al. Positron-emission tomography CT to identify local recurrence in stage I lung cancer patients 1 year after stereotactic body radiation therapy. *Strahlenther Onko*. 2013;189(6):495-501.
79. Dong X, Sun X, Sun L, et al. Early change in metabolic tumor heterogeneity during chemoradiotherapy and its prognostic value for patients with locally advanced non-small cell lung cancer. *PLoS One*. 2016;11(6): e0157836.
80. Carvalho S, Leijenaar RTH, Troost EGC, et al. Early variation of FDG-PET radiomics features in NSCLC is related to overall survival - the "delta radiomics" concept. *Radiat Oncol*. 2016;118:S20-S21.
81. Takeda A, Kunieda E, Fujii H, et al. Evaluation for local failure by 18F-FDG PET/CT in comparison with CT findings after stereotactic body radiotherapy (SBRT) for localized non-small-cell lung cancer. *Lung cancer*. 2013;79(3):248-253.
82. Mattonen SA, Palma DA, Haasbeek CJ, Senan S, Ward AD. Early prediction of tumor recurrence based on CT texture changes after stereotactic ablative radiotherapy (SABR) for lung cancer. *Med Phys*. 2014;41(3):033502.
83. Mattonen SA, Palma DA, Johnson C, et al. Detection of local cancer recurrence after stereotactic ablative radiation therapy for lung cancer: physician performance versus radiomic assessment. *Int J Radiat Oncol Biol Phys*. 2016;94(5):1121-1128.
84. Moran A, Daly ME, Yip SSF, Yamamoto T. Radiomics-based assessment of radiation-induced lung injury after stereotactic body radiotherapy. *Clin Lung Cancer*. 2017;18(6):e425-e431
85. Fave X, Zhang L, Yang J, et al. Delta-radiomics features for the prediction of patient outcomes in non-small cell lung cancer. *Sci Rep*. 2017;7(1):588.
86. Chong Y, Kim JH, Lee HY, et al. Quantitative CT variables enabling response prediction in neoadjuvant therapy with EGFR-TKIs: are they different from those in neoadjuvant concurrent chemoradiotherapy? *PLoS One*. 2014;9(2): e88598.
87. Paul J, Yang C, Wu H, et al. Early assessment of treatment responses during radiation therapy for lung cancer using quantitative analysis of daily computed tomography. *Int J Radiat Oncol Biol Phys*. 2017;98(2):463-472.
88. Mattonen SA, Ward AD, Palma DA. Pulmonary imaging after stereotactic radiotherapy—does RECIST still apply? *Br J Radiol*, 2016;89(1065):20160113.
89. van Timmeren JE, Leijenaar RTH, van Elmpt W, Reymen B, Lambin P. Feature selection methodology for longitudinal cone-beam CT radiomics. *Acta oncologica*. 2017;56(11):1537-1543.
90. Cunliffe A, Armato SG IIIrd, Castillo R, Pham N, Guerrero T, Al-Hallaq HA. Lung texture in serial thoracic computed tomography scans: correlation of radiomics-based features with radiation therapy dose and radiation pneumonitis development. *Int J Radiat Oncol Biol Phys*. 2015;91(5):1048-1056.
91. Bogowicz M, Riesterer O, Bundschuh RA, et al. Stability of radiomic features in CT perfusion maps. *Phys Med Biol*. 2016; 61(24):8736-8749.
92. Salamekh S, Rong Y, Ayan AS, et al. Inter-fraction tumor volume response during lung stereotactic body radiation therapy correlated to patient variables. *PLoS One*. 2016;11(4): e0153245.
93. Cunliffe AR, Contee C, Armato SG, IIIrd, et al. Effect of deformable registration on the dose calculated in radiation therapy planning CT scans of lung cancer patients. *Med Phys*. 2015; 42(1):391-399.
94. Maes F, Collignon A, Vandermeulen D, Marchal G, Suetens P. Multi-modality image registration by maximization of mutual information. 1996:14-22.
95. Larue RT, Defraene G, De Ruysscher D, Lambin P, van Elmpt W. Quantitative radiomics studies for tissue characterization: a review of technology and methodological procedures. *Br J Radiol*. 2017;90(1070):20160665.
96. Maurer CR, Fitzpatrick JM. A review of medical image registration. *Interactive Imageguided Neurosurgery*. 1995:17-44.
97. Oliveira FP, Tavares JM. Medical image registration: a review. *Comput Methods Biomech Biomed Engin*. 2014;17(2):73-93.
98. Cunliffe AR, Al-Hallaq HA, Labby ZE, et al. Lung texture in serial thoracic CT scans: assessment of change introduced by image registration. *Med Phys*. 2012;39(8):4679-4690.
99. Cunliffe AR, Armato SG III rd, Fei XM, Tuohy RE, Al-Hallaq HA. Lung texture in serial thoracic CT scans: registration-based methods to compare anatomically matched regions. *Med phys*. 2013;40(6):061906.
100. Benedict SH, Hoffman K, Martel MK, et al. Overview of the American Society For Radiation Oncology-National Institutes Of Health-American Association Of Physicists In Medicine Workshop 2015: exploring opportunities for radiation oncology in the era of big data. *Int J Radiat Oncol Biol Phys*. 2016;95(3): 873-879.